

Ballbot-type motion of N-heterocyclic carbenes on gold surfaces

Gaoqiang Wang^{1,2,3}, Andreas Rühling⁴, Saeed Amirjalayer^{1,2,5}, Marek Knor^{1,2}, Johannes Bruno Ernst⁴, Christian Richter⁴, Hong-Jun Gao³, Alexander Timmer^{1,2}, Hong-Ying Gao^{1,2}, Nikos L. Doltsinis^{5,6}, Frank Glorius^{4*} and Harald Fuchs^{1,2,5*}

Recently, N-heterocyclic carbenes (NHCs) were introduced as alternative anchors for surface modifications and so offered many attractive features, which might render them superior to thiol-based systems. However, little effort has been made to investigate the self-organization process of NHCs on surfaces, an important aspect for the formation of self-assembled monolayers (SAMs), which requires molecular mobility. Based on investigations with scanning tunnelling microscopy and first-principles calculations, we provide an understanding of the microscopic mechanism behind the high mobility observed for NHCs. These NHCs extract a gold atom from the surface, which leads to the formation of an NHC-gold adatom complex that displays a high surface mobility by a ballbot-type motion. Together with their high desorption barrier this enables the formation of ordered and strongly bound SAMs. In addition, this mechanism allows a complementary surface-assisted synthesis of dimeric and hitherto unknown trimeric NHC gold complexes on the surface.

Surface modifications, in particular on gold, have been used during the past three decades to achieve significant breakthroughs in fields such as nanotechnology¹, sensing², surface protection and microelectronics³. The majority of these advances were realized by using thiol-based ligands because of their critical ability to create self-assembled monolayers (SAMs). A comparatively new but promising alternative is the class of N-heterocyclic carbenes (NHCs), which are already known to be excellent ligands for metal complexes and nanoparticles^{4,5}. The great potential of NHC ligands becomes clear when looking at key catalysts in the fields of metathesis^{6,7}, cross coupling⁸ and asymmetric hydrogenation⁹. NHCs are strong σ -donating and moderately π -accepting ligands¹⁰, which renders them especially suitable binders for the late-transition metals such as gold¹¹. So far, only three reports have explored the use of NHCs for the modification of gold surfaces; they show that (1) NHCs bind to gold surfaces¹², (2) NHCs are stable enough to be modified further using a series of chemical reactions¹³ and (3) NHCs can form ultrastable SAMs on surfaces that withstand chemical stress¹⁴.

Despite the great importance of these contributions, they all used different NHCs, which makes a comparison difficult. None of these works addressed the microscopic mechanisms of the molecular self-assembly process of the NHCs and their mobility after being deposited on the surface. Mobility is one of the inherent key features for a surface ligand to create a SAM, as this requires a mobile equilibrium between different binding modes on the surface.

As NHCs are strong binders, one would expect a negligible mobility on a surface, which, as shown herein, is not the case, but this seeming contradiction was also resolved in the present study. We believe that a systematic investigation of the mobility of NHCs on surfaces will help to improve the quality of SAMs and

other related surface modifications, which can be beneficial to improve the physical and chemical properties of materials. Here we present a systematic study on the mobility of a set of representative NHCs on gold and the related mechanism via scanning tunnelling microscopy (STM) analysis in combination with first principles calculations^{15,16}.

Results and discussion

To obtain reliable data for the mobility and its mechanism, we envisioned physical vapour deposition of the NHCs on the surface under ultrahigh vacuum (UHV) conditions to be a higher-quality method^{17,18} in comparison with the previously used wet-deposition approach^{12–14}. We see the core problem of this method in the residual salt and solvent impurities, which lead to a lower-quality surface and the resulting analysis (for example, the STM images). Therefore, we switched from the usual NHC salt to the NHC carboxylates, which are considered to be masked free NHCs, as they cleanly generate a free NHC under heating (liberating CO₂) (Fig. 1a) and were previously used in a wet-deposition approach for the formation of NHC monolayers on gold^{13,19}. We chose three NHCs, IMes, IPr and IMe (Fig. 1b), for our investigations, because they are analogous to previously studied NHCs on surfaces and all well represented in homogeneous applications, and they differ in their stability and steric and electronic properties, which could be important for their mobility on a surface^{12–14}. By heating the CO₂ adduct of IMes in UHV, IMes was installed on the gold surface in a directly bound fashion without any impurities derived from the NHC precursor. However, no ordered structure but rather ellipsoidal shapes of differently oriented single IMes molecules could be observed (Fig. 1c). A free molecular rotation on the surface can be excluded in this case because free rotating molecules would appear circular in the

¹Physikalisches Institut, Westfälische Wilhelms-Universität, Wilhelm-Klemm-Straße 10, 48149 Münster, Germany. ²Center for Nanotechnology, Heisenbergstraße 11, 48149 Münster, Germany. ³Institute of Physics & University of Chinese Academy of Sciences, Chinese Academy of Sciences, PO Box 603, Beijing 100190, China. ⁴Organisch-Chemisches Institut, Westfälische Wilhelms-Universität Münster, Corrensstrasse 40, 48149 Münster, Germany. ⁵Center for Multiscale Theory and Computation, Westfälische Wilhelms-Universität Münster, Wilhelm-Klemm-Straße 10, 48149 Münster, Germany. ⁶Institut für Festkörpertheorie, Westfälische Wilhelms-Universität Münster, Wilhelm-Klemm-Straße 10, 48149 Münster, Germany.

*e-mail: glorius@uni-muenster.de; fuchsh@uni-muenster.de

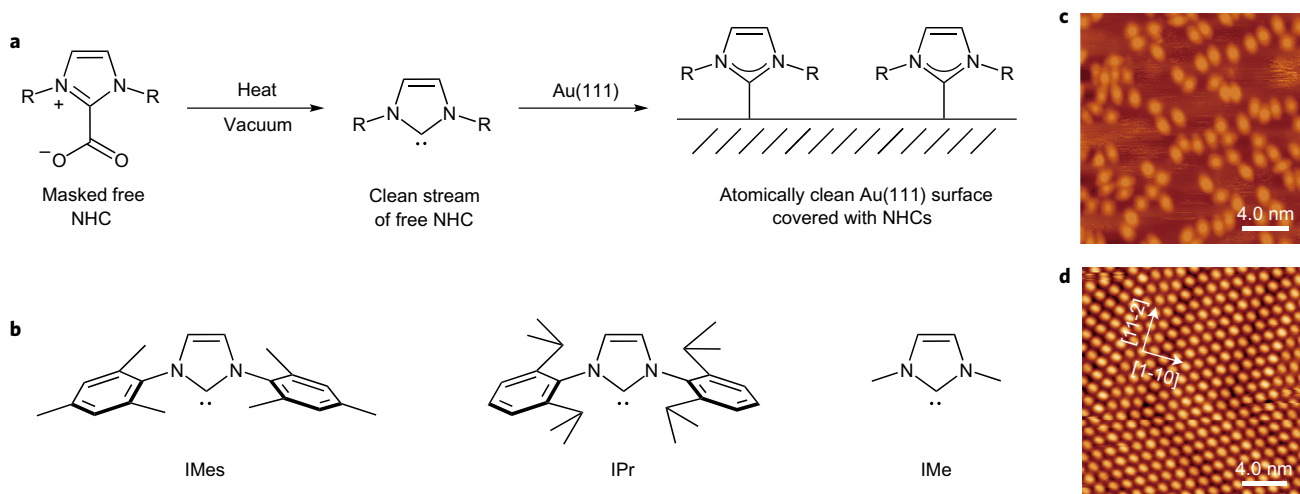


Figure 1 | Investigated NHCs and STM images of NHCs on Au surfaces. **a**, Schematic illustration of the procedure used to install NHCs on gold by physical vapour deposition. **b**, The investigated NHCs. **c**, The STM image ($V = -2.2$ V, $I = 34$ pA) shows IMes directly bonded to a Au(111) surface. **d**, The STM image ($V = 2.73$ V, $I = 25$ pA) of IPr on Au(111) shows a highly ordered and dense hexagonally packed full monolayer.

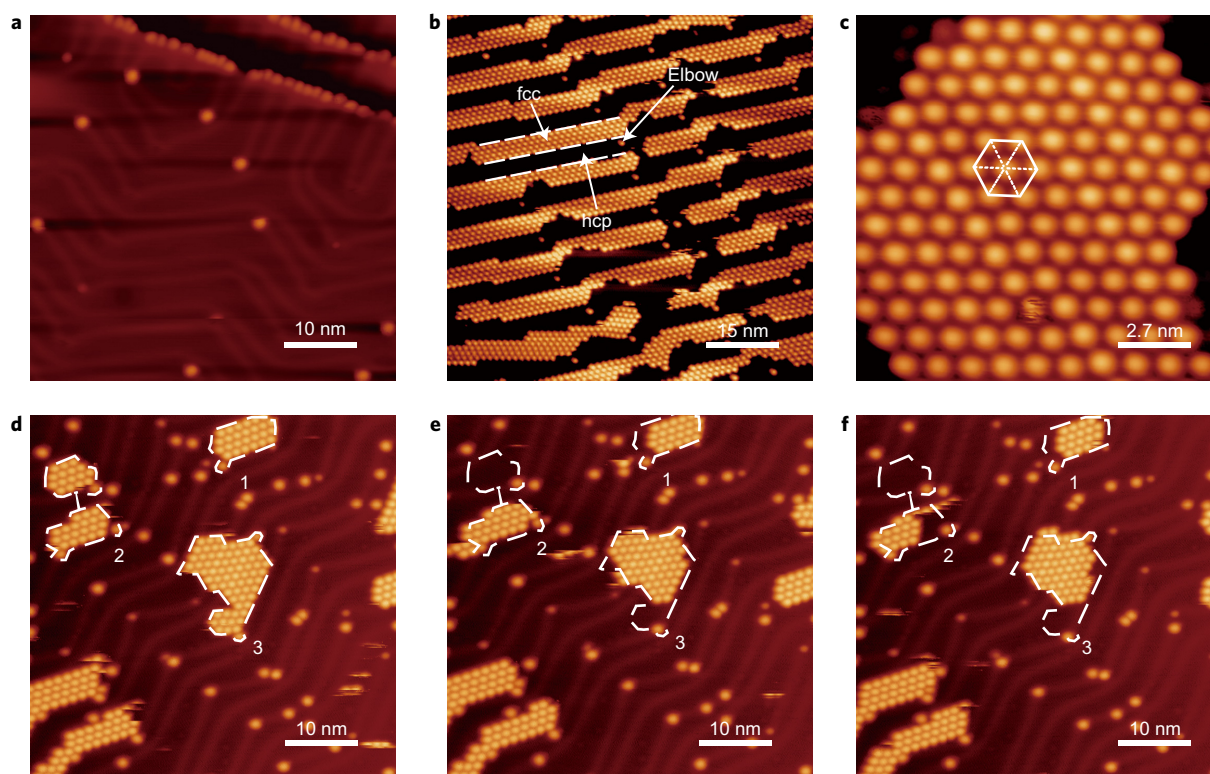


Figure 2 | STM topography images of IPr-Au. **a**, Low-coverage STM image ($V = -2.31$ V, $I = 23$ pA) that indicates rotation. **b**, Submonolayer STM image ($V = -1.94$ V, $I = 12$ pA) that shows IPr-Au preferentially occupying the fcc regions and elbow positions. The dashed lines indicate the domain walls of an Au(111) herringbone reconstruction. **c**, High-resolution STM image of an IPr-Au island that shows the hcp structure. A unit cell connecting four IPr-Au complexes with a distance of $a = 12.7 \pm 0.3$ Å is indicated. **d-f**, Successive scanning images ($V = -1.65$ V, $I = 13$ pA) taken in the same area. The evolution of the islands (white dashed lines) marked as 1, 2 and 3 indicates the mobility of IPr-Au islands on the Au(111) surface.

STM images²⁰. In sharp contrast to these results, a Au(111) surface was controllably covered with IPr and IMe via the same approach (Figs 1d and 2a,b for IPr and Supplementary Fig. 7 for IMe). X-ray photoelectron spectroscopy (XPS) analysis showed no traces of oxygen on the surface, which indicates that, indeed, the NHC, but not the CO₂ adduct, is binding (Supplementary Fig. 1). The absence of oxygen was additionally proved by direct-inlet mass spectrometry, which showed the decarboxylation at a pressure

of around $2.0\text{--}2.7 \times 10^{-7}$ mbar at 305 K. This is in favour of the NHC binding and against a binding of the NHC-CO₂ adduct (Supplementary Fig. 2).

At a very low surface coverage, up to 0.01 monolayer, IPr was observed along the edges of the Au(111) step and elbow positions of the $22 \times \sqrt{3}$ reconstructed Au(111) surface²¹ (Fig. 2a). This phenomenon is consistent with previous reports^{22,23}. When the coverage was increased above 0.05 monolayer, the formation of islands made of

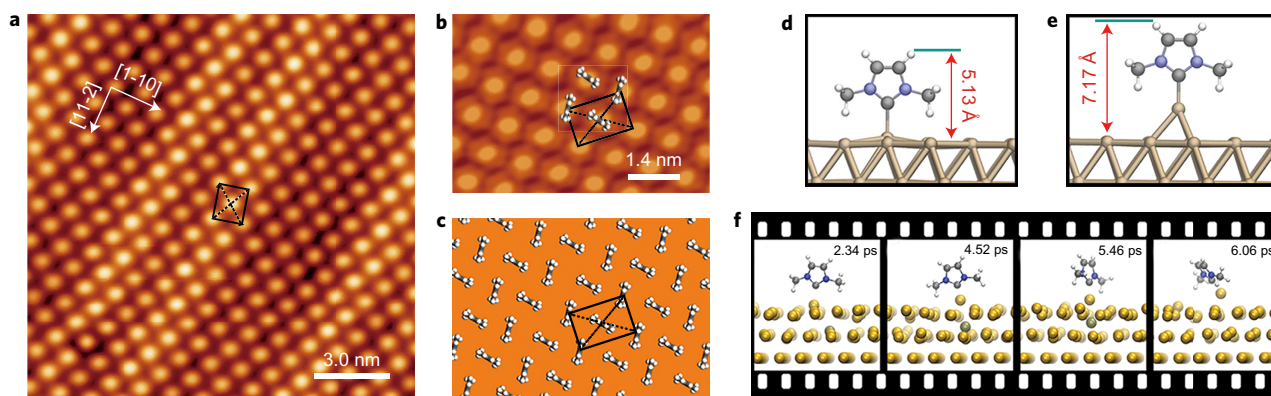


Figure 3 | Densely packed film of IMe-Au on the Au(111) surface and the DFT results. **a**, STM image ($V = -0.6$ V, $I = 21$ pA) of IMe-Au on Au(111). A unit cell with a distance of $a = 11.5 \pm 0.3$ Å and $b = 15.7 \pm 0.3$ Å is indicated. **b**, High-resolution STM image ($V = -0.45$ V, $I = 15$ pA) of IMe-Au that shows a centred rectangular close-packed structure. **c**, Schematic of IMe-Au on the Au(111) surface. **d,e**, Geometric structures of IMe on Au(111) without (**d**) and with (**e**) an additional Au adatom as determined from DFT optimization. **f**, Snapshots from a CP-MD simulation of IMe on Au(111) (Supplementary Movie 1) illustrate the extraction of an Au atom from the top layer and the concerted migration of an Au atom in the second layer (dark-shaded ball) to fill the vacancy in the top layer.

IPr could be observed, which preferentially occupy face-centred-cubic (fcc) stacking regions^{24,25} (Fig. 2b). In contrast with the previous reports, we found that these islands easily break up into smaller units and eventually recombine on the surface (Fig. 2d–f), without influencing the occurrence of the herringbone reconstruction²⁶. Even at the saturation coverage, the sample still exhibits mobility (Supplementary Fig. 5) and the herringbone structure of the Au (111) substrate underneath²⁵ together with a hexagonal-close-packed (hcp) structure is observed (Figs 1d and 2c). Despite the high on-surface mobility, the adsorbed molecules are stable to high temperatures (Supplementary Fig. 6), which underlines the stability of the obtained SAMs. Under the experimental conditions ($T \approx 77$ K), IPr appears as a round shape on Au(111) (Fig. 2a and Supplementary Fig. 3), indicating free rotation around a single bond between the NHC carbon and an Au atom^{20,27,28}. At first glance, these observations appear to contradict the general assumption that the NHC binds strongly to the gold surface, leading to a dense and rigid film. However, this behaviour can be explained easily by a NHC-induced adatom formation, in which the NHC sticks to its adatom and uses this to ‘travel’ the surface in a ballbot-type motion²⁹. Adatom formation has been discussed mainly in the context of thiol deposition^{30,31}, and speculated about for NHCs⁵. This is supported by the work of Johnson and co-workers, who calculated that an IMes derivative bound to a single Au atom on top of a small Au cluster is the lowest energy scenario¹³. The adatom formation can be verified by comparing the height of IPr-Au at different positions (Supplementary Fig. 4), where IPr denotes the NHC alone and IPr-Au stands for a single NHC bound to a single Au adatom. At the islands, the molecules are elevated by about 2.4 Å higher above the surface than in some other positions. This indicates that not all Au NHC complexes are directly bonded to the surface, but the majority of them are bound via an adatom to the surface.

To gain a better understanding of the mechanism, we also performed STM measurements with IMe on Au(111). At low coverage, IMe-Au shows a similar behaviour to that of IPr-Au (Supplementary Fig. 7a). With increasing coverage, however, differences are observed (Supplementary Fig. 7b,c). At the saturation coverage, IMe-Au forms a centred rectangular close-packed structure (Fig. 3a,b). We attribute these differences to the influence of varied substituents at the nitrogen atoms. To strengthen our hypothesis of a molecular ballbot-like motion, we conducted static and dynamic density functional theory (DFT) calculations on IMe. DFT calculations revealed the rotational barrier to be 15 meV, which is accessible at temperatures of or below 77 K and reflects the conditions under

which the experiment was conducted. The likelihood of this type of motion becomes clear when we look at the optimized adsorption geometry (Fig. 3d,e). That the gold atom covalently connected to IMe is lifted above the surface by 0.32 Å (the total height between the backbone hydrogen atoms and the gold surface is 5.13 Å) is evidence of the strong effect that IMe exerts on the gold surface. In this configuration, IMe is strongly bound to a single Au atom at the top site, which is the most stable position (Supplementary Fig. 9a). A dynamical treatment using Car–Parrinello molecular dynamics (CP–MD) reveals that the adsorbing Au atom is easily extracted fully from the surface to create a transient vacancy, which is, however, simultaneously filled by an Au atom from the second Au layer in a concerted process (Fig. 3f). The simulations further show that once the adatom is formed, the NHC diffuses rapidly across the surface. Also, the adatom formation appears to be irreversible, that is, the surface Au layer subsequently remains intact and no vacancies are observed (Supplementary Movie 1 for an animation of the full CP–MD trajectory). We mention in passing that an analogous simulation for methanethiol did not show this phenomenon, which indicates a different mechanism for the mobility of thiol-based SAMs. In these systems, the sulfur prefers a threefold coordination at the hollow site, in contrast to the singly bonded NHC carbon, and adatom formation has only been seen under the influence of an external force³².

To back up quantitatively the observations made in the simulations, we have carried out free-energy calculations for the extraction of a single Au atom leading to the formation of an adatom. From a series of constrained CP–MD simulations followed by thermodynamic integration, a free-energy barrier of 12 kJ mol⁻¹ was obtained at 300 K. In a second series of simulations, we repeated the extraction process for a clean surface, that is, in the absence of IMe. This resulted in a free-energy barrier of 125 kJ mol⁻¹, one order of magnitude higher than that with the NHC. In addition, we calculated the activation barrier for surface diffusion of an Au adatom with and without IMe attached to it (Supplementary Fig. 9b,c). In both cases, the barrier is 10 kJ mol⁻¹, so the presence of IMe reduces the value only marginally. This numerical evidence clearly supports the notion that IMe is highly mobile on gold surfaces because of the formation of adatoms for which there is a low barrier to diffusion. In contrast to this, the energy barrier for the diffusion process without the Au adatom, that is, for IMe directly bonded to the surface, is significantly higher (77 kJ mol⁻¹). Furthermore, the diffusion pathway that involves desorption and re-adsorption of the Au-IME species is not accessible as a result of the high binding energy of 3.53 eV. To understand the effect of the side groups, we

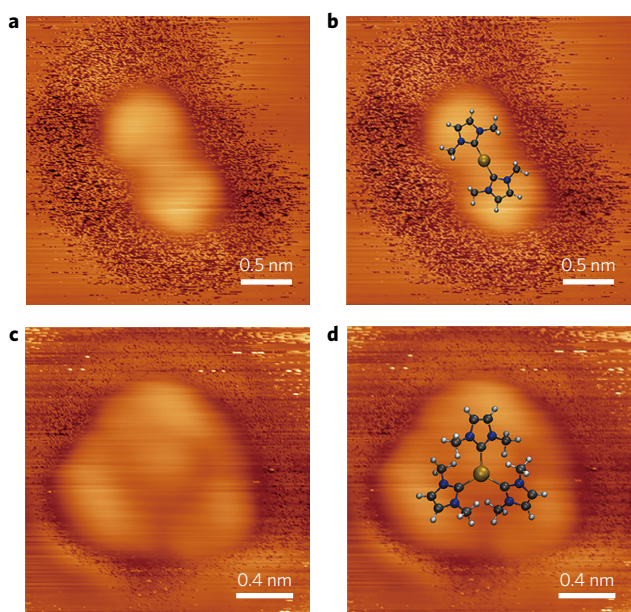


Figure 4 | Dimeric and trimeric gold complexes. **a**, STM image ($V = -1.77$ V, $I = 58$ pA) of a dimer formed by IMe. **b**, The same image as in **a** with a superimposed geometric structure from the DFT calculations. **c**, STM image ($V = -1.35$ V, $I = 19$ pA) of the trimer formed by IMe. **d**, The same image as in **c** with a superimposed geometric structure from the DFT calculations.

performed further DFT calculations on the larger NHCs, IPr and IMes, adsorbed on the Au surface (Supplementary Fig. 10). The binding energy increases in both cases because of the non-bonding interactions of the aromatic side groups with the surface. In the case of IMes, the binding energy increases by 1.6 eV compared with that of the parent molecule IMe. Comparing the optimized geometries of IPr and IMes, which differ by 0.59 eV in their binding energy (Supplementary Table 1), it can be seen that the more weakly binding IPr molecule pulls the Au atom out of the surface by ~ 0.2 Å further than the strongly interacting IMes, because of the stronger steric repulsion of the alkyl groups present in IPr. (Supplementary Fig. 10). As this process is the initial stage of the NHC–Au formation, the IPr is more likely to form such adatom complexes required for the high mobility. Based on our calculations, it can be reasoned that the potential of NHC molecules to pull out single Au atoms to form highly mobile NHC–Au species is governed by a delicate balance between electronic and steric effects. In addition, the very high binding energy of IMes explains its low mobility, as observed in the STM measurements (Fig. 1c).

As a consequence of its high mobility, IMe is not only able to form self-assembled aggregate structures, but also two additional chemical species, namely dimeric and trimeric NHC complexes, as we found in our STM studies (Fig. 4a–d and Supplementary Fig. 8). Both complexes were formed following an equilibration after the initial formation of the monolayer. A scenario in which an NHC dissociates from the surface and is re-deposited again is unlikely. As the gold atom of these complexes is an adatom, the interaction with the substrate might have caused a surface-assisted formation of the complexes and is one of the reasons for the stability. The formation of such complexes is truly remarkable, as to date the syntheses of zerovalent coinage metal–NHC complexes is very challenging. An exception are two reports of Bertrand *et al.*, who used cyclic (alkyl)aminocarbenes, the strongest σ -donating ligands made so far^{33,34}. Trimeric NHC complexes of the type $[\text{Au}(\text{NHC})_3]$ (here NHC = IMe), as observed in this study, have still not been reported. Related complexes of the type $[\text{Au}_n(\text{NHC})_{n+1}]^+$ were reported earlier by Monge, Guari and co-workers³⁵. This is

surprising as, according to our DFT calculations, trimeric complexes are inherently unstable in vacuum; however, they can be stabilized by the Au surface.

Conclusions

By using STM and first-principles simulations, we have solved the seemingly contradictory situation of the high mobility of NHCs on gold surfaces and provided a detailed characterization of the mechanism of NHC monolayer formation. Although binding strongly to the Au, NHCs can, indeed, move easily on surfaces via a unique ballbot-type motion, in which the NHC first pulls out an Au atom and then rides on it across the surface. This unique mode of mobility is key to the formation of SAMs and a surface-assisted synthesis of gold complexes on the surface. Further studies are in progress to investigate the mobility aspects discussed here in terms of the specific chemical nature of the NHCs as well as the possibilities to generate novel NHC–metal complexes on planar and nanostructured surfaces that cannot be generated by conventional liquid- or gas-phase chemistry, and which may display intriguing electronic and chemical properties. Our work provides a quantitative mechanistic understanding of the binding behaviour, mobility and stability of NHCs on metal surfaces under well-controlled conditions. We hope that this provides general insight into all kinds of systems of NHC–metal surface, including liquid–solid interfaces and etching effects.

Methods

Methods, along with some other additional display items, are available in the Supplementary Information.

Received 4 January 2016; accepted 22 August 2016;
published online 3 October 2016

References

- Love, J. C., Estroff, L. A., Kriebel, J. K., Nuzzo, R. G. & Whitesides, G. M. Self-assembled monolayers of thiolates on metals as a form of nanotechnology. *Chem. Rev.* **105**, 1103–1169 (2005).
- Nuzzo, R. G. & Allara, D. L. Adsorption of bifunctional organic disulfides on gold surfaces. *J. Am. Chem. Soc.* **105**, 4481–4483 (1983).
- Veisheh, M., Wickes, B. T., Castner, D. G. & Zhang, M. Guided cell patterning on gold–silicon dioxide substrates by surface molecular engineering. *Biomaterials* **25**, 3315–3324 (2004).
- Hopkinson, M. N., Richter, C., Schedler, M. & Glorius, F. An overview of N-heterocyclic carbenes. *Nature* **510**, 485–496 (2014).
- Zhukhovitskiy, A. V., MacLeod, M. J. & Johnson, J. A. Carbene ligands in surface chemistry: from stabilization of discrete elemental allotropes to modification of nanoscale and bulk substrates. *Chem. Rev.* **115**, 11503–11532 (2015).
- Vougioukalakis, G. C. & Grubbs, R. H. Ruthenium-based heterocyclic carbene-coordinated olefin metathesis catalysts. *Chem. Rev.* **110**, 1746–1787 (2010).
- Fortman, G. C. & Nolan, S. P. N-Heterocyclic carbene (NHC) ligands and palladium in homogeneous cross-coupling catalysis: a perfect union. *Chem. Soc. Rev.* **40**, 5151–5169 (2011).
- Kantchev, E. A. B., O'Brien, C. J. & Organ, M. G. Palladium complexes of N-heterocyclic carbenes as catalysts for cross-coupling reactions—a synthetic chemist's perspective. *Angew. Chem. Int. Ed.* **46**, 2768–2813 (2007).
- Zhao, D., Candish, L., Paul, D. & Glorius, F. N-heterocyclic carbenes in asymmetric hydrogenation. *ACS Catal.* **6**, 5978–5988 (2016).
- Jacobsen, H., Correa, A., Poater, A., Costabile, C. & Cavallo, L. Understanding the M(NHC) (NHC = N-heterocyclic carbene) bond. *Coord. Chem. Rev.* **253**, 687–703 (2009).
- Marion, N., Ramon, R. S. & Nolan, S. P. [(NHC)Au(i)]-catalyzed acid-free alkyne hydration at part-per-million catalyst loadings. *J. Am. Chem. Soc.* **131**, 448–449 (2009).
- Weidner, T. *et al.* NHC-based self-assembled monolayers on solid gold substrates. *Aust. J. Chem.* **64**, 1177–1179 (2011).
- Zhukhovitskiy, A. V., Mavros, M. G., Van Voorhis, T. & Johnson, J. A. Addressable carbene anchors for gold surfaces. *J. Am. Chem. Soc.* **135**, 7418–7421 (2013).
- Crudden, C. M. *et al.* Ultra stable self-assembled monolayers of N-heterocyclic carbenes on gold. *Nat. Chem.* **6**, 409–414 (2014).
- Diaz Arado, O. *et al.* On-surface azide–alkyne cycloaddition on Au(111). *ACS Nano* **7**, 8509–8515 (2013).
- Zhong, D. *et al.* Linear alkane polymerization on a gold surface. *Science* **334**, 213–216 (2011).

17. Griffiths, M. B. E. *et al.* Surfactant directed growth of gold metal nanoplates by chemical vapor deposition. *Chem. Mater.* **27**, 6116–6124 (2015).
18. Johnson, J. A. & Zhukhovitskiy, A. V. Articles and methods comprising persistent carbenes and related compositions. WO Patent WO2014160471A2 (2014).
19. Voutchkova, A. M., Feliz, M., Clot, E., Eisenstein, O. & Crabtree, R. H. Imidazolium carboxylates as versatile and selective N-heterocyclic carbene transfer agents: synthesis, mechanism, and applications. *J. Am. Chem. Soc.* **129**, 12834–12846 (2007).
20. Zhong, D., Wedeking, K., Chi, L., Erker, G. & Fuchs, H. Surface-mounted molecular rotors with variable functional groups and rotation radii. *Nano Lett.* **9**, 4387–4391 (2009).
21. Barth, J. V., Brune, H., Ertl, G. & Behm, R. J. Scanning tunneling microscopy observations on the reconstructed Au(111) surface: atomic structure, long-range superstructure, rotational domains, and surface defects. *Phys. Rev. B* **42**, 9307–9318 (1990).
22. Voigtländer, B., Meyer, G. & Amer, N. M. Epitaxial growth of thin magnetic cobalt films on Au(111) studied by scanning tunneling microscopy. *Phys. Rev. B* **44**, 10354–10357 (1991).
23. Zhang, L. *et al.* Site- and configuration-selective anchoring of iron-phthalocyanine on the step edges of Au(111) surface. *J. Phys. Chem. C* **115**, 10791–10796 (2011).
24. Bo, M., Morgenstern, K., Schneider, W.-D., Berndt, R. & Wo, C. Self-assembly of 1-nitronaphthalene on Au(111). *Surf. Sci.* **444**, 199–210 (2000).
25. Xiao, W. D. *et al.* Impact of heterocirculene molecular symmetry upon two-dimensional crystallization. *Sci. Rep.* **4**, 5415 (2014).
26. Zhang, H. *et al.* Surface supported gold–organic hybrids: on-surface synthesis and surface directed orientation. *Small* **10**, 1361–1368 (2014).
27. Perera, U. G. *et al.* Controlled clockwise and anticlockwise rotational switching of a molecular motor. *Nat. Nanotechnol.* **8**, 46–51 (2013).
28. Gimzewski, J. K. *et al.* Rotation of a single molecule within a supramolecular bearing. *Science* **281**, 531–533 (1998).
29. Kumagai, M. & Ochiai, T. Development of a robot balancing on a ball. in *Int. Conf. Control, Automation and Systems* 433–438 (IEEE, 2008).
30. Maksymovych, P., Sorescu, D. C. & Yates, J. T. Jr. Gold-atom-mediated bonding in self-assembled short-chain alkanethiolate species on the Au(111) surface. *Phys. Rev. Lett.* **97**, 146103 (2006).
31. Gao, L. *et al.* Constructing an array of anchored single-molecule rotors on gold surfaces. *Phys. Rev. Lett.* **101**, 197209 (2008).
32. Nguyen, H. C., Szyja, B. M. & Doltsinis, N. L. Electric conductance of a mechanically strained molecular junction from first principles: crucial role of structural relaxation and conformation sampling. *Phys. Rev. B* **90**, 115440 (2014).
33. Weinberger, D. S. *et al.* Isolation of neutral mono- and dinuclear gold complexes of cyclic (alkyl)(amino)carbenes. *Angew. Chem. Int. Ed.* **52**, 8964–8967 (2013).
34. Jerabek, P., Roesky, H. W., Bertrand, G. & Frenking, G. Coinage metals binding as main group elements: structure and bonding of the carbene complexes [TM(cAAC)₂] and [TM(cAAC)₂]⁺ (TM = Cu, Ag, Au). *J. Am. Chem. Soc.* **136**, 17123–17135 (2014).
35. Crespo, J. *et al.* Ultrasmall NHC-coated gold nanoparticles obtained through solvent free thermolysis of organometallic Au(I) complexes. *Dalton Trans* **43**, 15713–15718 (2014).

Acknowledgements

Financial support from the Deutsche Forschungsgemeinschaft (DFG) through the SFB 858 (projects B02 and B15), the Transregional Collaborative Research Center TRR 61 (projects B03 and B07), the Ministry of Science and Technology of China (no. 2013CBA01600), the National Natural Science Foundation of China (no. 61390501), the Leibniz award (F.G.) and the Fonds der Chemischen Industrie (J.B.E.) is gratefully acknowledged. We also thank O. Diaz-Arado and H. Mönig (both Westfälische Wilhelms-Universität) for support with the sample preparation for the XPS measurements.

Author contributions

F.G. and H.F. initiated the project. F.G., H.F., G.W., A.R., S.A., N.D., M.K., J.B.E. and H.-Y.G. designed the experiments and coordinated the study. A.R., J.B.E. and C.R. synthesized the molecules. G.W. and M.K. performed the STM measurements. S.A. and N.D. performed DFT calculations. F.G., H.F., G.W., A.R., S.A., N.D., M.K., J.B.E., H.-J.G., H.-Y.G. and C.R. interpreted data. A.T. did the XPS experiments. H.F. and F.G. wrote the manuscript together with G.W., A.R., S.A. and N.D. All the authors read and commented on the manuscript.

Additional information

Supplementary information is available in the [online version of the paper](#). Reprints and permissions information is available online at www.nature.com/reprints. Correspondence and requests for materials should be addressed to F.G. and H.F.

Competing financial interests

The authors declare no competing financial interests.